Synergistic Antitumor Effects of Immune Cell-Viral Biotherapy

Steve H. Thorne *et al.*

Science **311**, 1780 (2006);
DOI: 10.1126/science.1121411

Science (print ISSN 0036-8075; online ISSN 1095-9203) is published weekly, except the last week in December, by the American Association for the Advancement of Science, 1200 New York Avenue NW, Washington, DC 20005.

female mice received a single injection of FCA, along with four injections of GFP-expressing CByB6F1spleen cells (5×10^5 per injection, administered over 2 weeks). Included was a control group of 12-week-old prediabetic NOD female mice that received a single injection of FCA alone. In both cases, all mice were protected from diabetes (fig. S4) (*7*). Moreover, intact islets, some with evidence of insulitis, were present in both groups of protected mice. However, we failed to detect GFP^+ cells by immunohistochemistry or Western blot analyses (Fig. 2B). In addition, spleen cells from GFP-treated mice retained the capacity to transfer diabetes into third-party NOD.scid recipients (fig. S5) (*7*).

In our experiments, no evidence of replacement of islets by the allogeneic spleen cells was observed. Moreover, immunological reaction to the injected cells was seen, as would be anticipated. Finally, the presence of diabetogenic T cells, albeit in a quiescent state, indicated that the abnormal autoimmune process persisted in these treated mice. It is likely that the normoglycemia observed in the four mice from the original protocol resulted from a few β cells that had survived the initial T cell attack and subsequently expanded to maintain blood glucose levels. Potentially, these could derive from precursor cells found in ducts or from surviving pre-existing β cells, which is consistent with a similar conclusion found in two recent studies (*11*, *12*). We also examined the pancreas of 14 diabetic mice maintained on insulin for 2 to 3 weeks, that is, under the same initial situation as the mice in the original protocol. We observed in this experiment a large variation in the number of surviving islets and β cells, with 3 of the 14 mice examined containing about 6% of the normal content of β cells and the rest having less (fig. S6A) (*7*). Most of the islets were abundant in glucagon-positive cells, although some cells were PDX-1 positive but negative for insulin (fig. S6B) (*7*). Thus, even in the presence of marked hyperglycemia, an indication of advanced diabetes, some β cells can survive for at least a period of time. It is possible that, as their insulin content decreases, the surviving β cells become less susceptible to attack by the insulin-specific T cells that dominate the immunological reaction (*13*–*15*). It is noteworthy that at the time of the first reading of hyperglycemia, the number of β cells was decreased by 71% in five mice examined. Between the time of the first evidence of hyperglycemia and the time the protocol was started [that is, 7 to 20 days (*2*, *3*)], there was a precipitous drop in islet β cell numbers. Along these lines, other studies demonstrated the successful reversion of disease with antibodies to CD3 or CD4 molecules, but only in newly diabetic NOD mice (*16*, *17*). In sum, the present findings in the 20% of mice displaying restored islet function when there is immunological regulation indicate that some β cells survived immunologic attack. Finding means of preserving these cells and stimulating their expansion could represent an exciting new approach to the prevention and treatment of T1DM.

References and Notes

1. R. Tisch, H. McDevitt, *Cell* **85**, 291 (1996).
2. S. Kodama, W. Kuhtreiber, S. Fujimura, E. A. Dale, D. L. Faustman, *Science* **302**, 1223 (2003).
3. S. Ryu, S. Kodama, K. Ryu, D. A. Schoenfeld, D. L. Faustman, *J. Clin. Invest.* **108**, 63 (2001).
4. M. W. Sadelain, H. Y. Qin, J. Lauzon, B. Singh, *Diabetes* **39**, 583 (1990).
5. D. Ulaeto, P. E. Lacy, D. M. Kipnis, O. Kanagawa, E. R. Unanue, *Proc. Natl. Acad. Sci. U.S.A.* **89**, 3927 (1992).
6. M. F. McInerney, S. B. Pek, D. W. Thomas, *Diabetes* **40**, 715 (1991).
7. Materials and methods are available as supporting material on *Science* Online.
8. A. Suri *et al.*, unpublished data.
9. L. C. Murtaugh, D. A. Melton, *Annu. Rev. Cell Dev. Biol.* **19**, 71 (2003).
10. A. Suri *et al.*, *Eur. J. Immunol.* **34**, 447 (2004).
11. J. Nishio, J. L. Gaglia, S. E. Turvey, C. Campbell, C. Benoist, D. Mathis, *Science* **311**, 1775 (2006).
12. A. S. Chong *et al.*, *Science* **311**, 1774 (2006).
13. D. R. Wegmann *et al.*, *J. Autoimmun.* **6**, 517 (1993).
14. D. R. Wegmann, M. Norbury-Glaser, D. Daniel, *Eur. J. Immunol.* **24**, 1853 (1994).
15. D. R. Wegmann, R. G. Gill, M. Norbury-Glaser, N. Schloot, D. Daniel, *J. Autoimmun.* **7**, 833 (1994).
16. L. Makhlouf *et al.*, *Transplantation* **77**, 990 (2004).
17. L. Chatenoud, E. Thervet, J. Primo, J. F. Bach, *Proc. Natl. Acad. Sci. U.S.A.* **91**, 123 (1994).
18. K. L. Johnson, D. K. Zhen, D. W. Bianchi, *Biotechniques* **29**, 1220 (2000).

19. This work was supported by a grant from the Juvenile Diabetes Research Foundation. We thank M. Levisetti and K. Polonsky for valuable suggestions and critical reading of the manuscript.

Supporting Online Material

www.sciencemag.org/cgi/content/full/311/5768/1778/DC1
Materials and Methods
Figs. S1 to S6
References

6 December 2005; accepted 10 February 2006
10.1126/science.1123500

Synergistic Antitumor Effects of Immune Cell-Viral Biotherapy

Steve H. Thorne,[1] Robert S. Negrin,[2] Christopher H. Contag[1]*

Targeted biological therapies hold tremendous potential for treatment of cancer, yet their use has been limited by constraints on delivery and effective tumor targeting. We combined an immune effector cell population [cytokine-induced killer (CIK) cells] with an oncolytic viral therapy to achieve directed delivery to, and regression of, tumors in both immunodeficient and immunocompetent mouse models. Preinfection of CIK cells with modified vaccinia virus resulted in a prolonged eclipse phase with the virus remaining hidden until interaction with the tumor. Whole-body imaging revealed that the cells retained their ability to traffic to and to infiltrate the tumor effectively before releasing the virus. These results illustrate the potential of combining biotherapeutics for synergistic effects that more effectively treat cancer.

A variety of immune cell–based cancer therapies have been proposed, many of which rely on the identification of tumor-associated antigens that are often weakly expressed on only a subset of tumor cells. Cytokine-induced killer (CIK) cells are a population of cells derived from human peripheral blood or mouse splenocytes after ex vivo expansion with interferon-γ, CD3-specific antibody, and interleukin-2 (*1*, *2*). They bear phenotypic markers of natural killer (NK) and T cells, express the receptor natural killer group 2D (NKG2D), and are not major histocompatibility complex (MHC)–restricted. Instead, they mediate killing of tumor cells through recognition of a class of stress-associated ligands expressed on the tumor cell surface (NKG2D ligands) (*3*). CIK cells, therefore, do not rely on one antigen. They have been shown to target a variety of tumors and can exert their cytotoxic effects following systemic delivery (*4*). Previous imaging studies in mice showed that, by 72 hours after intravenous delivery, CIK cells were localized primarily at the tumor site (*4*).

We reasoned that we could further functionalize the CIK cells by combining them with the enhanced tumor-killing capabilities of oncolytic viruses. Oncolytic viruses are replication-selective, or tropism-modified, viruses that complete a successful infection cycle only within transformed cells (*5*). The early success and lessons learned from first-generation adenovirus-based vectors, notably ONYX-015 (*6*), have led to the development of alternative oncolytic vectors based on other well-studied viruses, including

[1]Departments of Pediatrics, Radiology, Microbiology, and Immunology and [2]Department of Medicine and Division of Bone Marrow Transplantation, Stanford University School of Medicine, Stanford, CA 94305, USA.

*To whom correspondence should be addressed. E-mail: ccontag@cmgm.stanford.edu

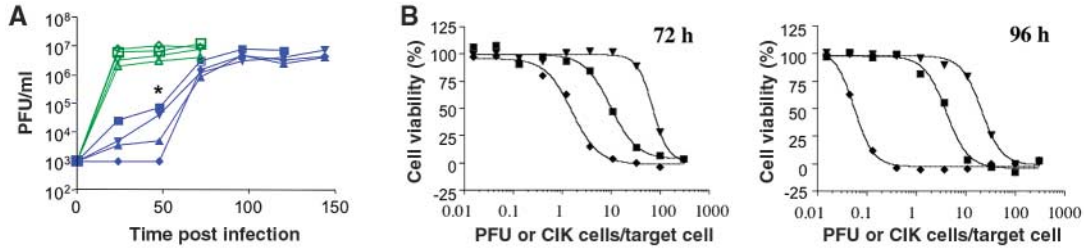

Fig. 1. Vaccinia virus displays unusual replication kinetics and increased cytopathic effect in human CIK cells. (**A**) Viral replication was followed for different vaccinia strains [WR (parental strain) (■); WR TK⁻ (▲); WR VGF⁻ (▼); vvDD (♦)] in human CIK cells (blue lines) and OCI-ly8 cells (human lymphoma, green lines) after infection at a multiplicity of infection (MOI) of 1.0 plaque-forming units (PFUs) per cell (* burst WR relative to vvDD in CIK; $P = 0.034$, t test). (**B**) Cytopathic effect on UCI-101 human ovarian cancer cell monolayers was measured in a cell viability assay at 72 and 96 hours after addition of different doses of human CIK cells (▼), vvDD (■), or preinfected CIK cells (♦). The replication of vaccinia in CIK is delayed, and preinfected CIK cells are more tumoricidal than either agent alone.

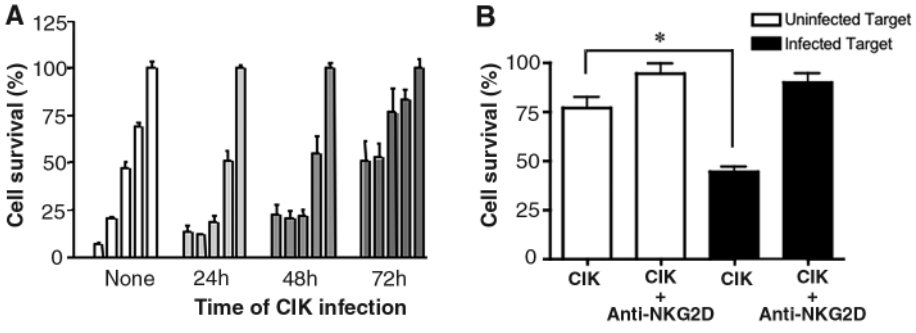

Fig. 2. In vitro interactions between human CIK cells, vvDD, and tumor cells. (**A**) Effects of preinfection on the cytolytic ability of CIK cells. UCI-101 target human ovarian tumor cells expressing luciferase were mixed with different numbers of CIK effector cells (ratios of 100:1, 50:1, 20:1, 10:1, and target only; left to right). CIK effector cells were uninfected (none) or preinfected with vvDD for 24, 48, or 72 hours. Luciferase output was measured as an indication of target cell survival after 4 hours. (**B**) Infected tumor cells display increased susceptibility to CIK cell killing. SKOV-3 target human ovarian tumor cells expressing luciferase, alone or preinfected with vvDD for 24 hours, were mixed with CIK cells at effector:target ratios of 20:1. In some experiments, CIK cells were premixed with NKG2D-blocking antibody. Luciferase signal was measured after 8 hours (*$P = 0.0076$, t test; error bars, SEM). Infected targets are killed more effectively by CIK cells; this success appears to be mediated by NKG2D on CIK cells and recognition of its ligands on the tumor target.

strains of poxviruses, such as vaccinia virus (*7*). Vaccinia, unlike most viruses proposed for use in virotherapy, has the advantage of systemic delivery potential and has a long history of use in humans, both during the smallpox eradication campaign and also as a tumor vaccine and oncolytic agent (*8*). However, because the virus infects many different cell types, only a small fraction of the inoculum of any strain used for virotherapy may reach the tumor, and this is likely to be further reduced in previously vaccinated individuals. Therefore, development of an effective means of delivering oncolytic viruses to tumor targets is needed. Here, using syngeneic and xenograft mouse models, we investigate the efficacy of a clinically relevant dual biotherapy that combines immune cell–mediated systemic delivery with the oncolytic ability of viruses.

We first determined the replication kinetics in human CIK cells of selected vaccinia virus strains and their parental strain (Western Reserve, WR). In contrast to the rapid and lytic replication seen in other cell lines such as the human lymphoma OCI-ly8 (Fig. 1A), all vaccinia strains displayed a two-step growth curve in CIK cells, with an initial extended eclipse period of slow replication followed by a rapid burst of replication 48 to 72 hours after infection. Poxviruses have been proposed to spread systemically after initial infection both as free virus and within infected hematopoietic cell populations (secondary viremia) (*9*), and these unusual replication kinetics may be characteristic of such spread. Deletion of the viral thymidine kinase (TK) gene restricts viral replication to cells in the G_2 and S phases of the cell cycle, during which the cells have elevated, compensatory levels of TK (*10*, *11*), and to cancer cells, where TK activity is constitutively high (*12*). TK-deleted vaccinia replicated both in the CIK cultures, where cell division was stimulated, and in tumor cells (Fig. 1A). The vaccinia viral growth factor (VGF) gene product promotes host cell growth after secretion from infected cells, by interacting with cellular growth factor receptors (*13*). VGF deletions restrict viral replication to cells with mutations in the Ras/mitogen-activated protein kinase/extracellular signal–regulated kinase (Ras/MAPK/ERK) pathway (*14*), offering additional tumor selectivity, while having a minimal effect on viral replication in CIK cells, which do not express growth factor receptors (Fig. 1A). A high degree of tumor selectivity, in culture and in vivo, has been demonstrated for a double-deleted vaccinia virus (vvDD) containing deletions in both TK and VGF (*15*). CIK cultures infected with vvDD produced almost no virus during the first 48 hours (Fig. 1A and fig. S1). Infection of human or mouse CIK cells with vvDD did not affect the expression of CIK phenotypic markers [CD3 and CD16/CD56 (human) or DX5 (mouse)] or NKG2D levels (fig. S2). In addition, infected CIK cells did not appear to present vaccinia antigens on their surface and were unaffected in their ability to produce interferon-γ (fig. S2). These data support the potential of CIK cells as carrier vehicles to deliver oncolytic vvDD to tumors.

We next investigated the interactions between CIK and tumor cells when either was infected with virus. vvDD-infected human CIK cells were highly effective for destroying human ovarian tumor cell monolayers in vitro (Fig. 1B), with a burst of cell killing between 72 and 96 hours after treatment. This correlated with the dispersal of virus from CIK cells onto the tumor cells instead of the slower cell-to-cell spread and plaque formation seen with virus alone (fig. S1B). When infected, CIK cells also retained their ability to kill the tumor targets (Fig. 2A).

CIK cells recognize NKG2D ligands on target cells (*3*), which are usually up-regulated under conditions of cellular stress, such as those encountered in the tumor microenvironment or after viral infection (*16*). Two of the best characterized NKG2D ligands in humans are MHC class I polypeptide-related sequences A and B (MICA and MICB) (*17*, *18*). We found that the surface expression levels of these proteins in the tumor cells directly correlated with their sensitivity to CIK cell–mediated killing (fig. S3). Furthermore, infection of the SKOV-3 cell line with vvDD virus resulted in an increase in the percentage of cells expressing MICA or MICB and increased the sensitivity of this

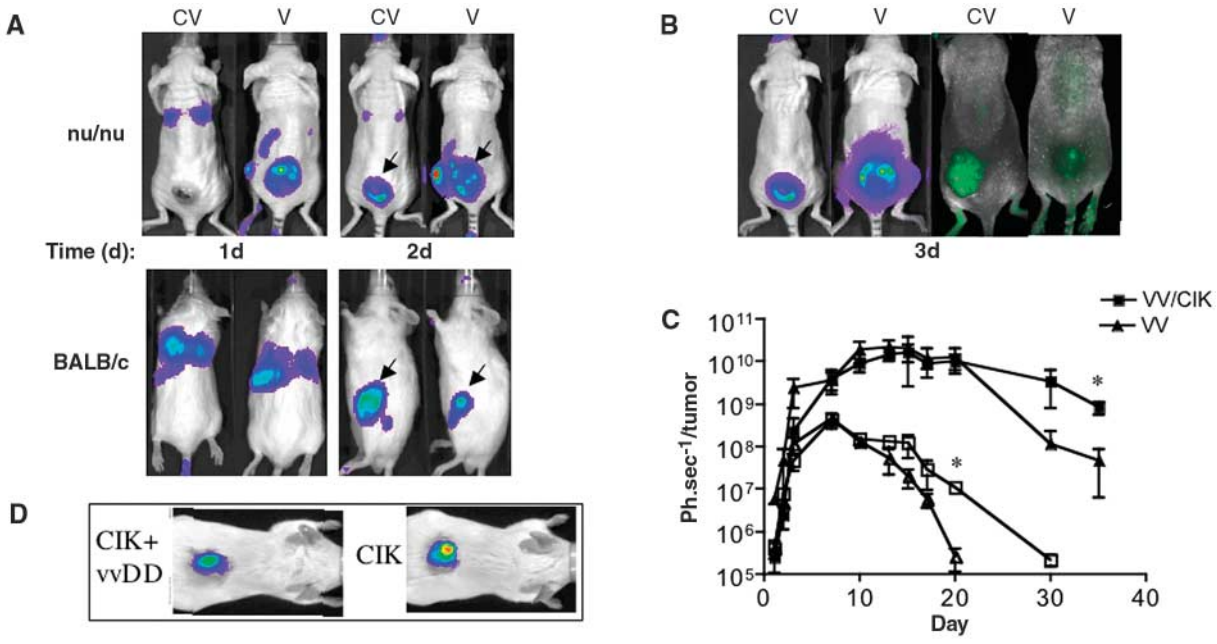

Fig. 3. Efficient trafficking of infected CIK cells to tumors improves delivery of oncolytic viruses. (**A**) Mice on the right received vvDD virus encoding luciferase alone (1×10^7 PFU; denoted V) or on the right in preinfected CIK cells (1×10^7 cells preinfected with virus at a multiplicity of infection of 1.0, 2 hours before delivery; denoted CV) via tail vein injection on day 0. Mice were imaged at the times indicated (in days post therapy) using an IVIS200 system (Xenogen Corp., Alameda, CA). nu/nu mice bearing UCI-101 xenograft human ovarian tumors (top) received human CIK cells; BALB/c immunocompetent mice bearing 4T1 murine mammary tumors (bottom) received murine CIK cells (arrows point to tumors). (**B**) At day 3 after treatment, bioluminescent and fluorescent signals were imaged. Mice were treated as before, but some received vvDD encoding green fluorescent protein (right panels), and all were imaged using a spectral unmixing camera (Maestro, CRI Ltd., Woburn, MA) to detect fluorescent signals and to demonstrate uniform distribution in tumors after viral delivery in CIK cells and nonuniform distribution in tumors where virus was given alone. (**C**) Quantification of bioluminescence output per tumor is plotted over time as an indication of viral gene expression for mice treated with vvDD or CIK cells preinfected with vvDD. Values are averages for three animals per group, error bars are SEM; $P = 0.0079$ for nu/nu mice (closed symbols) (day 35) and $P = 0.0089$ for BALB/c mice (open symbols) (day 20) (*t* test). (**D**) BALB/c mice bearing 4T1 murine mammary tumors were treated with murine CIK cells labeled with Cy5.5 dye, alone or after vvDD preinfection. Fluorescence imaging 72 hours after tail delivery was performed using an IVIS200 system. CIK-mediated delivery was more uniform than virus only, and preinfection did not prevent CIK trafficking to tumors.

otherwise resistant tumor cell to CIK-mediated killing ($P = 0.0076$), an effect that was reversed by addition of NKG2D-blocking antibody (Fig. 2B).

To investigate the in vivo trafficking of preinfected CIK cells to tumors and the subsequent biodistribution of virus, we used noninvasive optical imaging. Human CIK cells were used in immunodeficient mice with xenografts of human ovarian tumors, and murine CIK cells were used in immunocompetent mice with murine breast cancers. Although vaccinia replicates to significantly lower levels in mouse cells, the immunocompetent models allow the study of trafficking in the presence of an intact immune system. Luciferase-labeled vvDD and bioluminescence imaging revealed the distribution and duration of viral gene expression (Fig. 3). At 24 hours after injection, we observed the same pattern of viral gene expression within the lung, liver, and spleen, regardless of viral delivery method. However, the ratios were different. Virus delivered alone produced signal predominantly in the spleen, whereas virus within CIK cells produced signal predominantly in the lungs. Although the systemic delivery potential of vaccinia to tumors has been described previously (*15*, *19*), we observed a delay in detectable tumor signal following intravenous delivery of virus alone in immunocompetent mice compared with immunodeficient animals. By comparison, the use of preinfected CIK cells to deliver virus to the tumor resulted in the same patterns of viral biodistribution regardless of immune status or species of CIK origin (Fig. 3, A and B), with very little virus detected in any organ other than the tumor by 48 hours after treatment. The two delivery methods produced equivalent levels of viral gene expression from the tumor by 3 days after treatment (Fig. 3, B and C). Signals in the immunocompetent mice were weaker and began to decline earlier because of poor replication in murine cell lines and clearance by the immune response. Signal from CIK cell–delivered virus was sustained within the tumor for longer periods of time compared with signals for virus alone (Fig. 3C).

Labeling of CIK cells, by conjugation to a fluorescent dye (Cy5.5) or with luciferase, before intravenous delivery enabled visualization of cells at the tumor site (Fig. 3D and fig. S4). Preinfection with vvDD did not affect the trafficking of CIK cells to syngeneic or xenograft tumor models, confirming that the CIK cells carry the virus to the tumor. When mice bearing CIK-resistant SKOV-3 tumors were treated, accumulation of CIK cells was not observed in the tumor unless they were infected with vvDD virus (fig. S4), and this accumulation was found to colocalize to regions of the tumor where MICA or MICB had been up-regulated by vvDD infection (fig. S5). Also, it was found that, whereas vvDD delivered alone initially infected only tumor cells surrounding the vasculature, vvDD-infected CIK cells were capable of carrying the virus into the tumor mass and away from the vasculature (fig. S6). This produced more uniform distribution of viral infection within the tumor, which would likely contribute to sustained viral gene expression and increased tumor destruction in vivo.

To investigate the in vivo efficacy of the combination therapy, we first treated immunodeficient mice bearing xenografts of human ovarian tumor cell lines (Fig. 4A). Mice bearing established peritoneal tumors were treated with a single tail vein injection of each therapy. CIK cells alone were able to extend the median survival of mice bearing UCI-101 tumors by 8 days but had no effect on mice bearing the CIK-resistant SKOV-3 tumors. vvDD virus alone

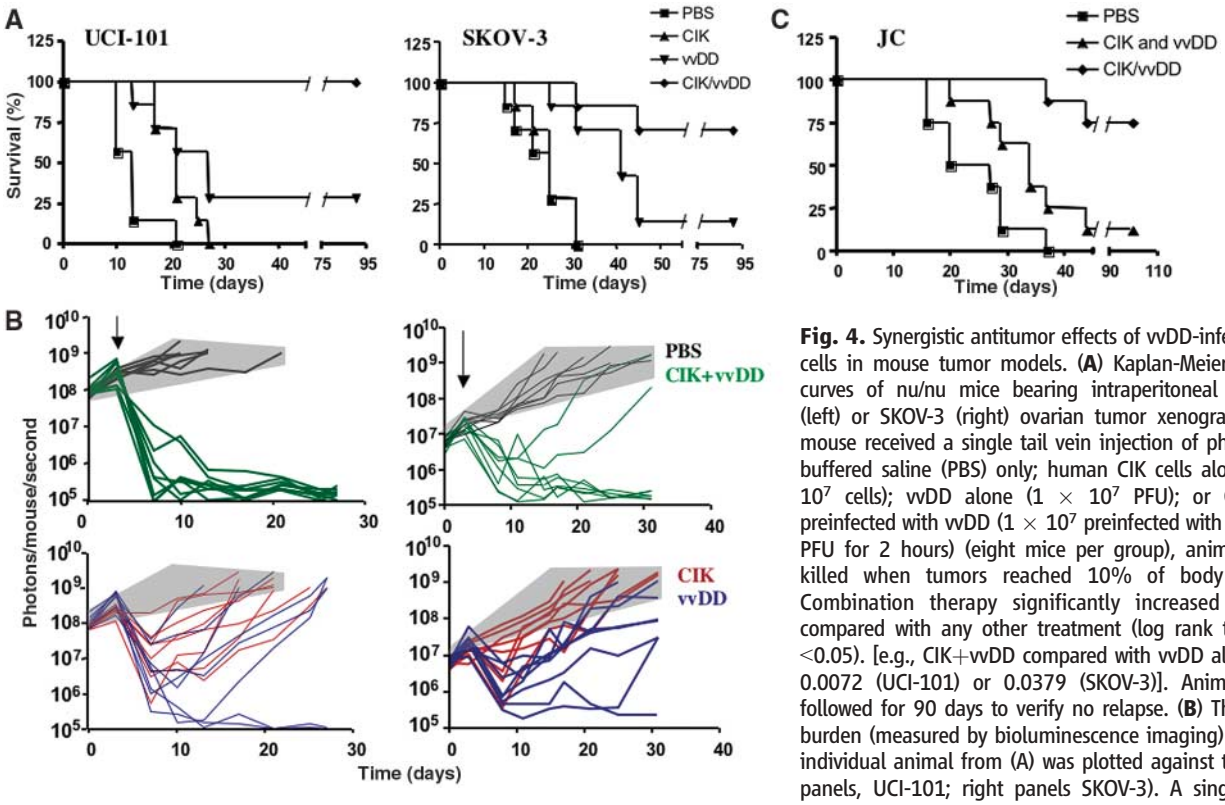

Fig. 4. Synergistic antitumor effects of vvDD-infected CIK cells in mouse tumor models. (**A**) Kaplan-Meier survival curves of nu/nu mice bearing intraperitoneal UCI-101 (left) or SKOV-3 (right) ovarian tumor xenografts. Each mouse received a single tail vein injection of phosphate-buffered saline (PBS) only; human CIK cells alone (1×10^7 cells); vvDD alone (1×10^7 PFU); or CIK cells preinfected with vvDD (1×10^7 preinfected with 1×10^7 PFU for 2 hours) (eight mice per group), animals were killed when tumors reached 10% of body weight. Combination therapy significantly increased survival compared with any other treatment (log rank test; $P = <0.05$). [e.g., CIK+vvDD compared with vvDD alone; $P = 0.0072$ (UCI-101) or 0.0379 (SKOV-3)]. Animals were followed for 90 days to verify no relapse. (**B**) The tumor burden (measured by bioluminescence imaging) for each individual animal from (A) was plotted against time (left panels, UCI-101; right panels SKOV-3). A single intravenous treatment was delivered on day 3 (arrows). Gray shaded area indicates range of tumor burden for the PBS-treated group. (**C**) Survival curves of immunocompetent BALB/c mice bearing murine breast cancer JC tumors (implanted into the fat pad, treated when 50 to 100 mm^3) after a single intravenous treatment with PBS alone; both murine CIK cells and vvDD were delivered separately; versus CIK cells preinfected with vvDD. The last-mentioned therapy significantly increased survival compared with the two therapies delivered separately ($P = 0.0046$) and control animals ($P < 0.0001$) (log rank test).

also increased median survival in both mouse models (by 15 to 16 days), with some animals (<30%) showing complete responses (Fig. 4A). In contrast, the combination therapy produced significantly increased survival compared with either therapy alone ($P < 0.01$). Mice bearing UCI-101 tumors showed a 100% complete response rate. The combination therapy also displayed a 62% increase in complete responses against SKOV-3 tumors compared with just the vvDD vector ($P = 0.0379$), despite the fact that the CIK cells alone had no effect against these tumors. Plots of the tumor burden in individual animals (Fig. 4B) indicated that single vvDD or human CIK cell therapy against sensitive tumors produced an initial response but that the tumors subsequently relapsed. Mice with complete responses were followed for up to 90 days with no evidence of tumor relapse or any toxicities attributable to the therapy. As the immune response is a major limitation to the delivery of viruses to tumors, the same experiment was repeated in immunocompetent mice bearing murine breast cancers. Mice bearing breast adenocarcinoma JC tumors implanted into the mammary fat pad (tumors 50 to 100 mm^3) were either treated with a single tail vein injection of preinfected CIK cells or with both CIK cells and vvDD delivered separately but on the same day (Fig. 4C). One mouse (of eight) treated with the individual therapies showed a complete response, whereas mice treated with preinfected CIK cells showed a much higher incidence of complete response (six out of eight), which demonstrated that preinfection is essential for the synergistic effects of the combined therapy. Similar results were seen in immunocompetent mice bearing the highly aggressive 4T1 mammary tumor cell lines (fig. S7). Although less than half the U.S. population has been vaccinated against smallpox, and most vaccinations took place over 30 years ago, there is evidence that immunity is long-lasting (*20*), and this may limit the effectiveness of this therapy. However, immunity is measured against naked virus, and so it is possible that infected CIK cells, which do not appear to present viral antigens (fig. S2B), may evade an immune response.

In conclusion, the benefits of exploiting naturally occurring biological phenomena in the treatment of disease are well known. Here we exploit the ability of certain viruses to conceal themselves within hematopoietic cells in order to take advantage of natural tumor trafficking of some immune cells to deliver a virus efficiently to the tumor. Cole *et al.* (*21*) recently reported that T cells targeted to an artificial antigen could deliver a nonreplicating, retroviral gene therapy vector to a tumor transformed to express the target antigen, which demonstrated the use of immune cells to deliver agents to tumor targets. However, because the therapeutic use of cells with a specific T cell receptor has been limited by a lack of suitable tumor antigens and the ability of many tumors to inhibit T cell activity (*22*) and because retroviral gene therapy vectors have been withdrawn from clinical trials after insertional mutagenesis led to serious adverse events (*23*), the clinical utility of this approach is unclear. Each of the therapies in the current report has shown some success in the clinic (*24*, *25*), and their demonstrated synergy now offers the potential of a targeted, biological therapy with systemic delivery, minimal toxicities and significant antitumor effects that could translate directly to the treatment of patients.

References and Notes

1. P. H. Lu, R. S. Negrin, *J. Immunol.* **153**, 1687 (1994).
2. J. Baker, M. R. Verneris, M. Ito, J. A. Shizuru, R. S. Negrin, *Blood* **97**, 2923 (2001).
3. M. R. Verneris, M. Karami, J. Baker, A. Jayaswal, R. S. Negrin, *Blood* **103**, 3065 (2004).
4. M. Edinger *et al.*, *Blood* **101**, 640 (2003).
5. D. Kirn, R. L. Martuza, J. Zwiebel, *Nat. Med.* **7**, 781 (2001).
6. C. Heise *et al.*, *Nat. Med.* **3**, 639 (1997).
7. S. H. Thorne, T. Hermiston, D. Kirn, *Semin. Oncol.* **32**, 537 (2005).
8. S. H. Thorne, D. H. Kirn, *Expert Opin. Biol. Ther.* **4**, 1307 (2004).

9. R. M. Buller, G. J. Palumbo, *Microbiol. Rev.* **55**, 80 (1991).
10. R. M. Buller, G. L. Smith, K. Cremer, A. L. Notkins, B. Moss, *Nature* **317**, 813 (1985).
11. M. Puhlmann *et al.*, *Cancer Gene Ther.* **7**, 66 (2000).
12. M. Hengstschlager *et al.*, *J. Biol. Chem.* **269**, 13836 (1994).
13. R. M. Buller, S. Chakrabarti, B. Moss, T. Fredrickson, *Virology* **164**, 182 (1988).
14. A. A. Andrade *et al.*, *Biochem. J.* **381**, 437 (2004).
15. J. A. McCart *et al.*, *Cancer Res.* **61**, 8751 (2001).
16. J. A. Hamerman, K. Ogasawara, L. L. Lanier, *Curr. Opin. Immunol.* **17**, 29 (2005).
17. S. Bauer *et al.*, *Science* **285**, 727 (1999).
18. V. Groh *et al.*, *Nat. Immunol.* **2**, 255 (2001).
19. Y. A. Yu *et al.*, *Nat. Biotechnol.* **22**, 313 (2004).
20. E. Hammarlund *et al.*, *Nat. Med.* **9**, 1131 (2003).
21. C. Cole *et al.*, *Nat. Med.* **11**, 1073 (2005).
22. G. P. Dunn, A. T. Bruce, H. Ikeda, L. J. Old, R. D. Schreiber, *Nat. Immunol.* **3**, 991 (2002).
23. S. Hacein-Bey-Abina *et al.*, *Science* **302**, 415 (2003).
24. T. Leemhuis, S. Wells, C. Scheffold, M. Edinger, R. S. Negrin, *Biol. Blood Marrow Transplant.* **11**, 181 (2005).
25. M. J. Mastrangelo *et al.*, *Cancer Gene Ther.* **6**, 409 (1999).
26. We thank W. Liang, L. Howe, and T. Doyle for their help with cell and animal imaging; J. Chan for cell lines; D. Bartlett for virus strains, Y.-A. Cao for retroviral vectors, and R. Critchley-Thorne and S. Schultz for help with the immunofluorescence microscopy studies. Supported by grants; NIH Small Animal Imaging Resource Program (SAIRP; R24 CA 92862), the Stanford Program Project Grant for Bone Marrow grafting for leukemia and lymphoma (P01 CA49605), the Molecular and Cellular Imaging Centers (ICMIC; P50 CA114747), and the John A. and Cynthia Fry Gunn Research Fund. All animal studies were performed according to Stanford University's Institutional Animal Care and Use Committee (IACUC)–approved protocols.

Supporting Online Material

www.sciencemag.org/cgi/content/full/311/5768/1780/DC1
Materials and Methods
Figs. S1 to S7
Reference

17 October 2005; accepted 2 March 2006
10.1126/science.1121411